Power Allocation and Transmission Mode Selection in Uplink D-MIMO ISAC Systems

Ezequias M. S. de Santana Jr., Pedro Victor M. Castro, Yuri C. B. Silva, Roberto P. Antonioli, Walter C. Freitas Jr., and Gábor Fodor

***Abstract*—Most integrated sensing and communication studies focus on downlink sensing, where base stations transmit sensing signals. In contrast, this work considers an uplink sensing scenario in a user-centric distributed multiple-input multiple-output centralized cloud radio access network, where users may simultaneously transmit sensing and communication signals. An integer optimization problem for transmission mode selection assigns each user to transmit only a communication signal or both communication and sensing signals with the goal of maximizing the communication sum-rate while satisfying minimum mainlobe-to-average-sidelobe-ratio constraints. This problem is solved via branch-and-bound and using heuristics based on the k-nearest neighbors and large-scale fading with equal and fractional power allocation. The numerical results show that optimal selection establishes an upper bound for sum-rate performance, whereas heuristics prioritize sensing performance at $\approx 22\%$ sum-rate cost, evidencing the need for joint power allocation and user selection.**

***Index Terms*—distributed multiple-input multiple-output, integrated sensing and communication, transmission mode selection.**

I. Introduction

Future sixth generation (6G) networks will support integrated sensing and communication (ISAC) to enable sensing capabilities alongside communication services, sharing resources to maximize efficiency [1]. Within this framework, multiple-input multiple-output (MIMO) architectures are essential for multi-target identification, while distributed topologies specifically exploit macro-diversity to provide better sensing reliability compared to monostatic approaches [2].

While monostatic ISAC architectures are constrained by self-interference and full-duplex requirements, conventional multistatic systems often need to deal with irregular coverage. To address these limitations, cell-free massive MIMO [3], [4] and distributed MIMO (D-MIMO) systems [5] leverage multiple transmission and reception points (TRPs) to improve sensing coverage while simultaneously enhancing communication performance. Furthermore, their multistatic topology inherently mitigates self-interference, eliminating the need for full-duplex hardware [6]. Since users, which are inherently engaged in communication, may also be simultaneously selected for sensing [5], joint power and user selection is essential to satisfy performance requirements while minimizing mutual interference.

Most research focuses on the downlink scenario, where the base station (BS) transmits to user equipment devices (UEs) while simultaneously probing a target or a spatial region [7]. In this context, the authors of [6] and [8] address joint power resource optimization for communication and sensing within multi-target detection frameworks. In [6], the authors propose a scalable framework enabling detection and target tracking based on the generalized likelihood ratio test. In contrast, the authors of [8] adopt a restrictive exclusive TRP selection strategy while jointly optimizing power allocation. In contrast, the authors of [5] consider an uplink (UL) cell-free network, in which UEs transmit both communication and sensing signals with fixed TRPs partitioned between communication and sensing,

This work was supported by: Ericsson Research, Sweden, and Ericsson Innovation Center, Brazil, under Technical Cooperation Contract UFC.52; CNPq under Grant 402569/2022-9; FUNCAP; FUNCAP/Universal Grant UNI-0210-00043.01.00/23; CAPES - Finance Code 001; CNPq/INCT-Signals Grant 406517/2022-3, and in part by the Swedish Strategic Research (SSF) grant for the FUS21-0004 SAICOM project.

E. M. S. de Santana Jr. (ORCID: 0009-0005-2671-0873), P. V. M. Castro (ORCID: 0009-0002-8214-5213), Y. C. B. Silva (ORCID: 0000-0002-1795-6004), R. P. Antonioli (ORCID: 0000-0003-1163-9953), and W. C. Freitas Jr. (ORCID: 0000-0002-0821-3460) are with the Wireless Telecom Research Group (GTEL), Department of Teleinformatics Engineering, Federal University of Ceará (UFC), Fortaleza, CE, Brazil (e-mail: {ezequias, pedrovictor, yuri, antonioli, walter}@gtel.ufc.br). G. Fodor (ORCID: 0000-0002-2289-3159) is with Ericsson Research, 16480 Stockholm, Sweden, and also with the KTH Royal Institute of Technology, 11428 Stockholm, Sweden (e-mail: gabor.fodor@ericsson.com).

Submission: 2026-04-24, First decision: 2026-06-24, Acceptance: 2026-11-11, Publication: 2026-11-16.

Digital Object Identifier: 10.14209/jcis.2026.18

evaluating beamforming strategies under heuristic power allocation. Conversely, [9] and [10] focuses on sensing parameter estimation in UL scenarios, but do not address a D-MIMO ISAC system.

Unlike the conventional downlink-based ISAC, UL ISAC enables the network to exploit the spatial distribution of the UEs as sensing transmitters. This letter investigates the sensing-communication trade-off and UEs selection for joint sensing and communication in a multistatic multi-target UL D-MIMO ISAC scenario. We formulate a UE transmission mode selection problem where each UE supports either joint sensing and communication or communication only. The goal is to select the best UEs for sensing, while maximizing the communication sum-rate under a sum-mainlobe-to-average-sidelobe-ratio (MASR) constraint.

II. System model

We consider a UL multistatic multi-target D-MIMO ISAC system under centralized cloud radio access network comprising K UEs, with N antennas each, and $Q = M + R$ TRPs, with L antennas each. The TRPs are divided into sets of M communication receivers (CRXs) and R sensing receivers (SRXs). Let $\mathcal{K}_{\mathrm{s}} \subseteq \mathcal{K}$ denote the subset of UEs performing sensing using shared time-frequency resources, with $\mathcal{K}$ representing the set of all UEs. Let $\mathcal{T}$ denote the set of all $T = |\mathcal{T}|$ targets and $\mathcal{T}_k \subseteq \mathcal{T}$ represent the set of targets served by the k-th UE. Each UE k either transmits communication symbols or jointly transmits communication and sensing signals to CRXs and SRXs sets, $\mathcal{M}_k^{\mathrm{c}}$ and $\mathcal{M}_k^{\mathrm{s}}$, respectively, where, $\mathcal{M}_k = \mathcal{M}_k^{\mathrm{c}} \cup \mathcal{M}_k^{\mathrm{s}}$.

The channel between the k-th UE and the m-th CRX, $\mathbf{H}_{m,k} \in \mathbb{C}^{L\times N}$, is non-line-of-sight and follows the Weichselberger model with correlated Rayleigh fading [11], [12], incorporating path-loss and correlated shadowing [13] via the coefficient $\beta_{m,k}$. The sensing channel is line-of-sight and accounts for the propagation between the k-th UE, the t-th target, and the r-th SRX. The azimuth and elevation angle pairs $(\varphi_{k,t}, \vartheta_{k,t})$ and $(\varphi_{r,t}, \vartheta_{r,t})$ denote the angular position of the t-th target relative to the k-th UE and the r-th SRX, respectively. Accordingly, the sensing channel path is modeled as $\mathbf{A}_{r,k,t} = \sqrt{\beta_{r,k,t}}\mathbf{a}_L(\varphi_{r,t}, \vartheta_{r,t})\mathbf{a}_N^T(\varphi_{k,t}, \vartheta_{k,t})$ where $\mathbf{a}_L(\cdot)$ and $\mathbf{a}_N(\cdot)$ are the three-dimensional uniform linear array (ULA) responses with half-wavelength antenna spacing, and $\beta_{r,k,t}$ denotes the bistatic path gain [4], [14], with the aggregated sensing coefficient defined as $\beta_{k,t} = \sum_{r\in\mathcal{M}_k^s} \beta_{r,k,t}$.

As in [3], we consider a time-division duplexing protocol with a coherence block length τ_c divided into τ_u UL transmission symbols and τ_p UL pilots. In the channel estimation phase, it is assumed that each UE transmits orthogonal pilot sequences of length $\tau_p \geq NK$ to avoid pilot contamination, without interference from the sensing service, as commonly considered in the literature [3], [12], [15].

After channel estimation, the signal transmitted by the k-th UE in the l-th time slot is given by

$$\mathbf{x}_k[l] = \sqrt{\rho_k}\mathbf{f}_k s_k[l] + \delta_k \sum_{t=1}^{T} \sqrt{\rho_{k,t}}\mathbf{f}_{k,t} s_{k,t}[l] \in \mathbb{C}^{N\times 1}, \tag{1}$$

where $\mathbf{f}_k$ and $\mathbf{f}_{k,t}$ are the communication and sensing precoders, respectively. Moreover, $s_k[l]$ and $s_{k,t}[l]$ denote the independent unit energy communication symbol and sensing signal intended for target t, respectively. Note that beamforming is used rather than spatial multiplexing, as this work focuses on transmission mode selection.

The binary variable δ_k models the transmission mode selection of the k-th UE. Specifically, when $\delta_k = 1$, the UE simultaneously transmits communication symbols and sensing signals, whereas when $\delta_k = 0$, it transmits communication symbols only. In addition, ρ_k and $\rho_{k,t}$ denote the power allocated to communication and to sensing the t-th region, respectively, out of a total of T known sensing hotspot regions. Furthemore, each UE is subject to a maximum power budget $P_{\max}$.

Sensing and communication TRP selection is performed using distinct strategies. For sensing, the n_r SRXs closest to each sensing region t are selected to perform passive sensing, resulting in a total of $R \leq n_r T$ SRXs; since the network is aware of the sensing regions of interest, this approach is practical and readily implementable. In contrast, the communication clustering follows the dynamic cooperation clustering (DCC) approach proposed in [3]. Following the DCC approach, the CRXs serving the k-th UE are selected based on their large-scale fading coefficients [16]. This association is represented by the DCC matrix $\mathbf{D}_{m,k} \in \mathbb{C}^{L\times L}$, which equals $\mathbf{I}_L$ if the m-th CRX serves the k-th UE, and $\mathbf{0}_{L\times L}$ otherwise.

Considering centralized processing, let $\hat{\mathbf{H}}_{m,k} \in \mathbb{C}^{L\times N}$ denote the estimated channel between the k-th UE and the m-th CRX. The received signal at a given CRX consists of the superposition of the communication signals transmitted from all UEs, the sensing signals associated with the targets, and additive noise.

By collecting the signals received at all M CRXs, the aggregated received signal can be written as

$$\mathbf{y} = \sum_{k=1}^{K} \mathbf{H}_k \mathbf{x}_k + \mathbf{n} \in \mathbb{C}^{ML\times 1}, \tag{2}$$

where $\mathbf{y} = [\mathbf{y}_1^T, \ldots, \mathbf{y}_M^T]^T$ is the concatenation of the received signals from all CRXs, $\mathbf{n} = [\mathbf{n}_1^T, \ldots, \mathbf{n}_M^T]^T$ is the aggregated noise vector with $\mathbf{n}_m \sim \mathcal{N}_{\mathbb{C}}(\mathbf{0}_L, \sigma_n^2 \mathbf{I}_L)$, and $\mathbf{H}_k = [\mathbf{H}_{1,k}^T, \ldots, \mathbf{H}_{M,k}^T]^T \in \mathbb{C}^{ML\times N}$ denotes the stacked channel of the k-th UE.

Following [3], the symbol intended for the k-th UE is estimated at the central processing unit (CPU) as $\hat{s}_k = \mathbf{v}_k^H \mathbf{D}_k \mathbf{y}$, where $\mathbf{v}_k \in \mathbb{C}^{ML\times 1}$ is the first left singular vector of the estimated channel $\hat{\mathbf{H}}_k = [\hat{\mathbf{H}}_{1,k}^T, \ldots, \hat{\mathbf{H}}_{M,k}^T]^T$ and $\mathbf{D}_k = \mathrm{diag}\{\mathbf{D}_{k,1}, \ldots, \mathbf{D}_{k,M}\} \in \mathbb{C}^{ML\times ML}$ is a block-diagonal selection matrix. Thus, the achievable spectral efficiency lower bound of the k-th UE is [3]

$$\gamma_k = \frac{\tau_u}{\tau_c} \mathbb{E}\left\{ \log_2 \left(1 + \frac{\rho_k \left| \mathbf{v}_k^H \mathbf{D}_k \hat{\mathbf{H}}_k \mathbf{f}_k \right|^2}{I_k + E_k + \sigma_n^2 \|\mathbf{D}_k \mathbf{v}_k\|^2} \right) \right\}, \tag{3}$$

where $\mathbf{f}_k \in \mathbb{C}^{N\times 1}$ is the first right singular vector of $\hat{\mathbf{H}}_k$, and $I_k = \sum_{i=1, i\neq k}^{K} \rho_i |\mathbf{v}_k^H \mathbf{D}_k \hat{\mathbf{H}}_i \mathbf{f}_i|^2 + \sum_{j=1}^{K} \sum_{t=1}^{T} \delta_j^2 \rho_{j,t} |\mathbf{v}_k^H \mathbf{D}_k \hat{\mathbf{H}}_j \mathbf{f}_{j,t}|^2$, with $\mathbf{f}_{j,t} = \mathbf{a}_N(\varphi_{j,t}, \vartheta_{j,t})/\sqrt{N}$, represents the communication interference from other UEs and from sensing tasks, respectively. In (3), $E_k = \sum_{i=1}^{K} \rho_i \mathbf{v}_k^H \mathbf{D}_k \mathbf{C}_i' \mathbf{D}_k \mathbf{v}_k + \sum_{j=1}^{K} \sum_{t=1}^{T} \delta_j^2 \rho_{j,t} \mathbf{v}_k^H \mathbf{D}_k \mathbf{C}_{j,t}' \mathbf{D}_k \mathbf{v}_k$ denotes the channel estimation error component, where $\mathbf{C}_k' = \mathbb{E}\{\tilde{\mathbf{H}}_k \mathbf{f}_k s_k s_k^* \mathbf{f}_k^H \tilde{\mathbf{H}}_k^H\}$ and $\mathbf{C}_{j,t}' = \mathbb{E}\{\tilde{\mathbf{H}}_j \mathbf{f}_{j,t} s_{j,t} s_{j,t}^* \mathbf{f}_{j,t}^H \tilde{\mathbf{H}}_j^H\}$ are the error covariance matrices [12] $\in \mathbb{C}^{ML\times ML}$, with $\mathbf{H}_k = \hat{\mathbf{H}}_k + \tilde{\mathbf{H}}_k$, and the estimation error $\tilde{\mathbf{H}}_k$.

Considering that the k-th UE may or may not transmit sensing signals toward the T sensing regions through its transmit precoder $\mathbf{f}_{k,t}$, and that the main lobe of the sensing radiation pattern is steered toward the center of the sensing region, the MASR metric is introduced to quantify the radiation gain within a sensing region relative to the sidelobe gains of the resulting radiation pattern [8]. This metric is derived from the power contributions associated with the different lobes. Specifically, from (1), the average beam power towards the t-th sensing region from the k-th UE is given by $P_k(\varphi_{k,t}, \vartheta_{k,t}) = \mathbb{E}\{|\mathbf{a}_N^H(\varphi_{k,t}, \vartheta_{k,t}) \mathbf{x}_k|^2\}$, which leads to the MASR of the t-th region, given by:

$$\Gamma_t = \frac{\sum_{k=1}^{K} \delta_k^2 \rho_{k,t} N^2}{\sum_{k=1}^{K} \rho_k a_{k,t} + \sum_{k=1}^{K} \delta_k^2 \sum_{q=1, q\neq t}^{T} \rho_{k,q} b_{k,t,q}}, \tag{4}$$

where $a_{k,t} = \left| \mathbf{a}_N^H(\varphi_{k,t}, \vartheta_{k,t}) \mathbf{f}_k \right|^2$ denotes the gain associated with the communication task, while $b_{k,t,q} = \left| \mathbf{a}_N^H(\varphi_{k,t}, \vartheta_{k,t}) \mathbf{a}_N(\varphi_{k,q}, \vartheta_{k,q}) \right|^2$ accounts for the interference induced by sensing transmissions toward other regions. Note that the MASR yields a tractable sensing metric that serves as a surrogate function for detection performance [8].

III. Problem formulation

Determining the UEs that perform sensing simultaneously with communication is critical for performance since the transmission mode variable, δ_k for the k-th UE, contributes directly to the communication interference in (3) and the transmitted sensing gain in (4). Therefore, we formulate the transmission mode selection problem to determine the selection variables $\boldsymbol{\delta} = [\delta_1, \ldots, \delta_K]^T$ that maximize the system sum-rate while ensuring a minimum sensing quality Γ_{thr}:

$$\max_{\boldsymbol{\delta}\in\{0,1\}^K} \sum_{k=1}^{K} \gamma_k \quad \text{s.t.} \sum_{t=1}^{T} \Gamma_t \geq \Gamma_{\text{thr}}, \tag{5}$$

which is a communication-centric problem, since its objective is to maximize the sum-rate, while the sum-MASR is an aggregate constraint that characterizes the overall sensing performance.

Problem (5) can be optimally solved via branch-and-bound (BB), with an exponential worst-case complexity $\mathcal{O}(2^K)$ [17]. To address this, we introduce two heuristics for selecting the UEs that perform sensing: the k-nearest neighbors (KNN) approach, which selects the n_k closest UEs to sense each target, and the largest large-scale fading (LLSF) approach [16], which selects UEs based on the UE-target-SRX path. The heuristics do not guarantee optimality, but have polynomial worst-case

complexity $\mathcal{O}(TK^2)$ [18], as both require sorting K elements for each target.

Regarding power allocation, we consider two schemes determined by the transmission mode variable δ_k. The first strategy is based on equal power allocation (EPA), where the power for communication and sensing for a given UE k is defined as $\rho_k = P_{\max} - \delta_k|\mathcal{T}_k|P_{\max}/(|\mathcal{T}_k|+1)$ and $\rho_{k,t} = \delta_k P_{\max}/(|\mathcal{T}_k|+1)$, respectively, ensuring that if $\delta_k = 0$, all $P_{\max}$ is used for communication; if $\delta_k = 1$, $P_{\max}/(|\mathcal{T}_k|+1)$ is allocated to communication and the $|\mathcal{T}_k|$ targets.

We also propose a conditional fractional power control (CFPC) strategy. When $\delta_k = 0$, $\rho_{k,t} = 0$, $\forall t \in \mathcal{T}_k$ and the communication power is given by: $\rho_k = P_{\max}\left(\sum_{m\in\mathcal{M}_k}\beta_{m,k}\right)^{\mu_c} / \max_{i\in\mathcal{S}_k}\left(\sum_{m\in\mathcal{M}_i}\beta_{m,i}\right)^{\mu_c}$, where $\mathcal{S}_k = \{i : \mathbf{D}_k\mathbf{D}_i \neq \mathbf{0}\}$ denotes the set of UEs that are partially served by the same TRPs as the UE k [3]. When $\delta_k = 1$, the UE transmitting powers are given by: $\rho_k = P_{\max}c_k\Omega_k^{-1}\sum_{m\in\mathcal{M}_k}\beta_{m,k}^{\mu_c}$; $\rho_{k,t} = \delta_k c_k'\beta_{k,t}^{\mu_s}P_{\max}\Omega_k^{-1}$where the normalization constants $c_k = \frac{1}{\max_m \beta_{m,k}^{\mu_c}}$ and $c_k' = \frac{1}{\max_t \beta_{k,t}^{\mu_s}}$ are introduced to limit large values related to the communication and aggregated sensing large-scale fading (LSF) coefficients $\beta_{m,k}$ and $\beta_{k,t}$, respectively [6], and $\Omega_k = c_k\sum_{m\in\mathcal{M}_k}\beta_{m,k}^{\mu_c} + c_k'\delta_k\sum_{t\in\mathcal{T}_k}\beta_{k,t}^{\mu_s}$.

The constants $\mu_c, \mu_s \in [-1, 1]$ represent the communication and sensing exponents that adjust the emphasis in both services, respectively [6]. Note that for these strategies, the k-th UE total allocated power will satisfy $\rho_k + \sum_{t=1}^{T}\rho_{k,t} \leq P_{\max}$.

IV. Results

We consider an Urban Micro scenario [13], in which the nodes are randomly and uniformly distributed over a 0.25 km^2 square area; a wrap-around technique was used for the receivers [3], and the targets are uniformly distributed within circular hotspots of radius 10 m each. The carrier frequency is 2 GHz, and the noise variance σ_n^2 is -94 dBm. The channels $\mathbf{H}_{m,k}$ are generated as in [12]. The correlated shadowing standard deviation and decorrelation distance are 4 dB and 9 m [13]. The target radar cross-section (RCS) variance [4] is 10 dBsm. The pilot, sensing and data power are set as $P_{\max} = 0.2$ W. The LSF follows [13], with 95% of its gain

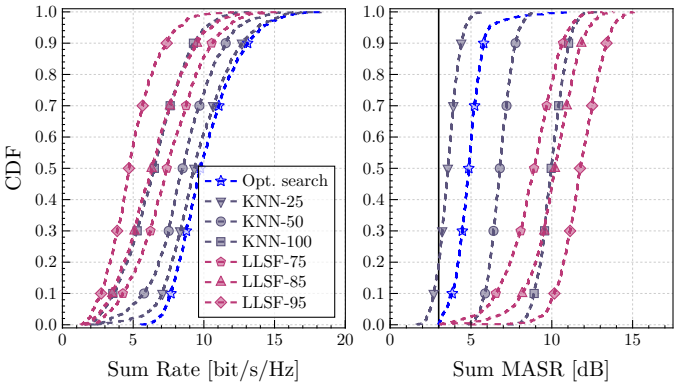


Figure 1. CDF of the EPA approach considering $\{Q, M, R, K, N, L, T\}$ = {16, 12, 4, 8, 4, 8, 2}; $\Gamma_{\text{thr}} = 3$ dB; $\{\tau_c, \tau_u, \tau_p\} = \{200, 168, 32\}$ symbols ; 1000 setups; 1000 Monte Carlo runs.

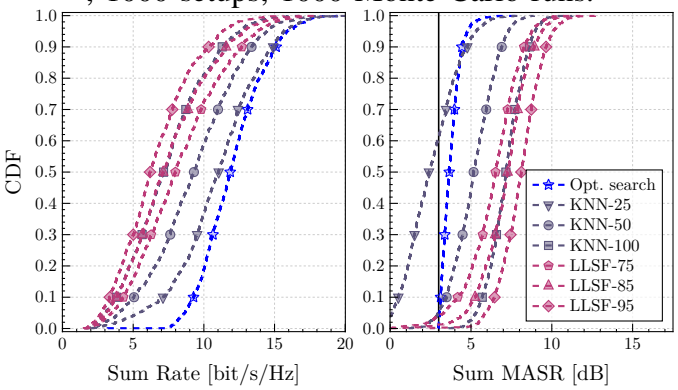


Figure 2. CDF of the CFPC approach for the same setup as in Fig. 1

.

considered for CRX association [16]. For the SRX, we considered $n_r = 2$, resulting in $R = 4$.

Figs. 1 and 2 present the cumulative distribution functions (CDFs) of the sum-rate and sum-MASR considering the EPA and CFPC, as well as five strategies for selecting the hybrid UEs. The Opt. search results are obtained by solving the optimization problem via BB; KNN-25, KNN-50 and KNN-100 are clustering-based heuristics using KNN, in which at most 25%, 50% and 100% of the UEs perform sensing, respectively; while the LLSF approaches LLSF-75, LLSF-85 and LLSF-95 select UEs for joint sensing and communication using LSF thresholds of 75%, 85% and 95%, respectively, with higher thresholds selecting more UEs [16]. The CFPC ($\mu_c = -0.5$, $\mu_s = 0.5$) configuration is adopted for the evaluations, as it was empirically observed to provide a favorable trade-off and closely tracks the EPA baseline.

As shown in Figs. 1 and 2, Opt. search delivers the highest sum-rate and satisfies the sum-MASR constraints, whereas the heuristic methods,

Table I
COMPARISON OF AVG. NUMBER OF HYBRID UES AND OUTAGE.

Algorithm	Avg. Hybrid UEs		Sens. Outage %	
	EPA	CFPC	EPA	CFPC
Opt. search	2.02	2.42	-	-
KNN-25	2.0	2.0	18.9	61.0
KNN-50	3.91	3.91	-	5.4
KNN-100	6.64	6.64	-	-
LLSF-75	5.49	5.49	-	3.9
LLSF-85	6.59	6.59	-	1.3
LLSF-95	7.77	7.77	-	0.3

especially in Fig. 2, do not. This occurs because BB is an exact method, whereas the heuristics are suboptimal methods. Also, the solutions that tend to maximize the sum-rate tend to reduce the values obtained from sum-MASR, which occurs because of the resource dispute between communication only ($\delta = 0$) and hybrid ($\delta = 1$) UEs, revealing a trade-off between the two services. In Fig. 1, almost all methods are feasible under EPA, while in Fig. 2 the CFPC does not guarantee feasibility for most heuristics, highlighting the conservative nature of EPA. Regarding CFPC, the heuristics under this power allocation achieve performance closer to the optimal solution. Yet, this sum rate gain comes at the cost of severe sensing outage for KNN-25.

Tab. I details the outage rates for each approach, corresponding to the point where the CDF curves cross the 3 dB threshold in Figs. 1 and 2. For CFPC, both the number of hybrid UEs and the transmission mode selection are critical to feasibility, as CFPC with BB or KNN-100 does not generate infeasible solutions. This can happen because outages may occur when the heuristics fail to select a feasible set of hybrid UEs, while CFPC does not guarantee that each UE uses its entire power budget. Tab. I also presents the average number of hybrid UEs, allowing to conclude that fewer hybrid UEs are associated with higher sum-rates due to reduced sensing interference and more UEs operating solely for communication.

V. CONCLUSION

This letter addressed the transmission mode selection problem and the inherent trade-off between sensing and communication in a multi-target UL D-MIMO ISAC scenario. The proposed BB approach provided a performance upper bound, achieving a median sum-rate gain of $\approx$ 3 bit/s/Hz over KNN heuristics, despite its complexity. Conversely, heuristic solutions provided better MASR performance at expense of $\approx 22\%$ median sum-rate loss between KNN-50 and the BB upper bound under fractional power allocation. Therefore, motivated by the presented trade-off, future research should explore joint power and transmission mode optimization to achieve better communication performance without compromising sensing constraints. Also, incorporating per-target constraints and extending the framework to multi-stream UEs are future topics, as it enables target-specific sensing requirements and spatial multiplexing, along with evaluating receiver-side sensing performance metrics such as detection probability, relating them to the MASR.

REFERENCES

[1] D. K. Pin Tan et al., "Integrated sensing and communication in 6G: Motivations, use cases, requirements, challenges and future directions," in *Proc. 1st IEEE International Online Symposium on Joint Communications & Sensing (JC&S)*, 2021, pp. 1–6. DOI: 10.1109/JCS52304.2021.9376324

[2] E. Fishler et al., "MIMO radar: An idea whose time has come," in *Proc. IEEE Radar Conference (IEEE Cat. No.04CH37509)*, 2004, pp. 71–78. DOI: 10.1109/NRC.2004.1316398

[3] Ö. T. Demir, E. Björnson, L. Sanguinetti, et al., "Foundations of user-centric cell-free massive MIMO," *Foundations and Trends® in Signal Processing*, vol. 14, no. 3-4, pp. 162–472, 2021. DOI: 10.1561/2000000109

[4] Z. Behdad et al., "Multi-static target detection and power allocation for integrated sensing and communication in cell-free massive MIMO," *IEEE Trans. Wireless Commun.*, vol. 23, no. 9, pp. 11 580–11 596, 2024. DOI: 10.1109/TWC.2024.3383209

[5] I. B. Palhano et al., "Power allocation for uplink sensing and communication in cell-free ISAC systems with multi-antenna users and multibeam," in *Proc. IEEE 100th Vehicular Technology Conference (VTC2024-Fall)*, 2024, pp. 1–5. DOI: 10.1109/VTC2024-Fall63153.2024.10757786

[6] S. Liesegang, S. Buzzi, and C. D'Andrea, "Scalable integrated sensing and communications for multi-target detection and tracking in cell-free massive MIMO: A unified framework," *IEEE Trans. Commun.*, vol. 74, pp. 2777–2793, 2025. DOI: 10.1109/TCOMM.2025.3642717

[7] C. Ouyang, Y. Liu, and H. Yang, "Performance of downlink and uplink integrated sensing and communications (ISAC) systems," *IEEE Wireless Commun. Lett.*, vol. 11, no. 9, pp. 1850–1854, 2022. DOI: 10.1109/LWC.2022.3184409

[8] M. Elfiatoure et al., "Multiple-target detection in cell-free massive MIMO-assisted ISAC," *IEEE Trans. Wireless Commun.*, vol. 24, no. 5, pp. 4283–4298, 2025. DOI: 10.1109/TWC.2025.3542206

[9] J. Bao et al., "Uplink networked sensing via multiuser correlation exploitation," 2026. arXiv: 2603.16442 [eess.SP].

[10] L. Zhao et al., "High-resolution uplink sensing in millimeter-wave ISAC systems," *IEEE Trans. Commun.*, vol. 73, no. 11, pp. 12 680–12 695, 2025. DOI: 10.1109/TCOMM.2025.3585582

[11] W. Weichselberger, M. Herdin, H. Ozcelik, and E. Bonek, "A stochastic MIMO channel model with joint correlation of both link ends," *IEEE Trans. Wireless Commun.*, vol. 5, no. 1, pp. 90–100, 2006. DOI: 10.1109/TWC.2006.1576533

[12] Z. Wang et al., "Uplink performance of cell-free massive MIMO with multi-antenna users over jointly-correlated Rayleigh fading channels," *IEEE Trans. Wireless Commun.*, vol. 21, no. 9, pp. 7391–7406, 2022. DOI: 10.1109/TWC.2022.3158353

[13] 3GPP, "Further advancements for E-UTRA physical layer aspects (release 9)," 3rd Generation Partnership Project (3GPP), Tech. Rep. 36.814, version 9.2.0, 2017.

[14] M. A. Richards, J. A. Scheer, and W. A. Holm, *Principles of Modern Radar: Basic Principles*. The Institution of Engineering and Technology, 2010. DOI: 10.1049/SBRA021E

[15] R. Pinto Antonioli et al., "On the energy efficiency of cell-free systems with limited fronthauls: Is coherent transmission always the best alternative?" *IEEE Trans. Wireless Commun.*, vol. 21, no. 10, pp. 8729–8743, Oct. 2022. DOI: 10.1109/TWC.2022.3169114

[16] H. Q. Ngo et al., "On the total energy efficiency of cell-free massive MIMO," *IEEE Trans. Green Commun. Netw.*, vol. 2, no. 1, pp. 25–39, 2018. DOI: 10.1109/TGCN.2017.2770215

[17] G. L. Nemhauser and L. A. Wolsey, *Integer and Combinatorial Optimization*. New York, NY, USA: John Wiley & Sons, 1988. DOI: 10.1002/9781118627372

[18] T. H. Cormen, C. E. Leiserson, R. L. Rivest, and C. Stein, *Introduction to Algorithms*, 3rd ed. Cambridge, MA, USA: MIT Press, 2009.